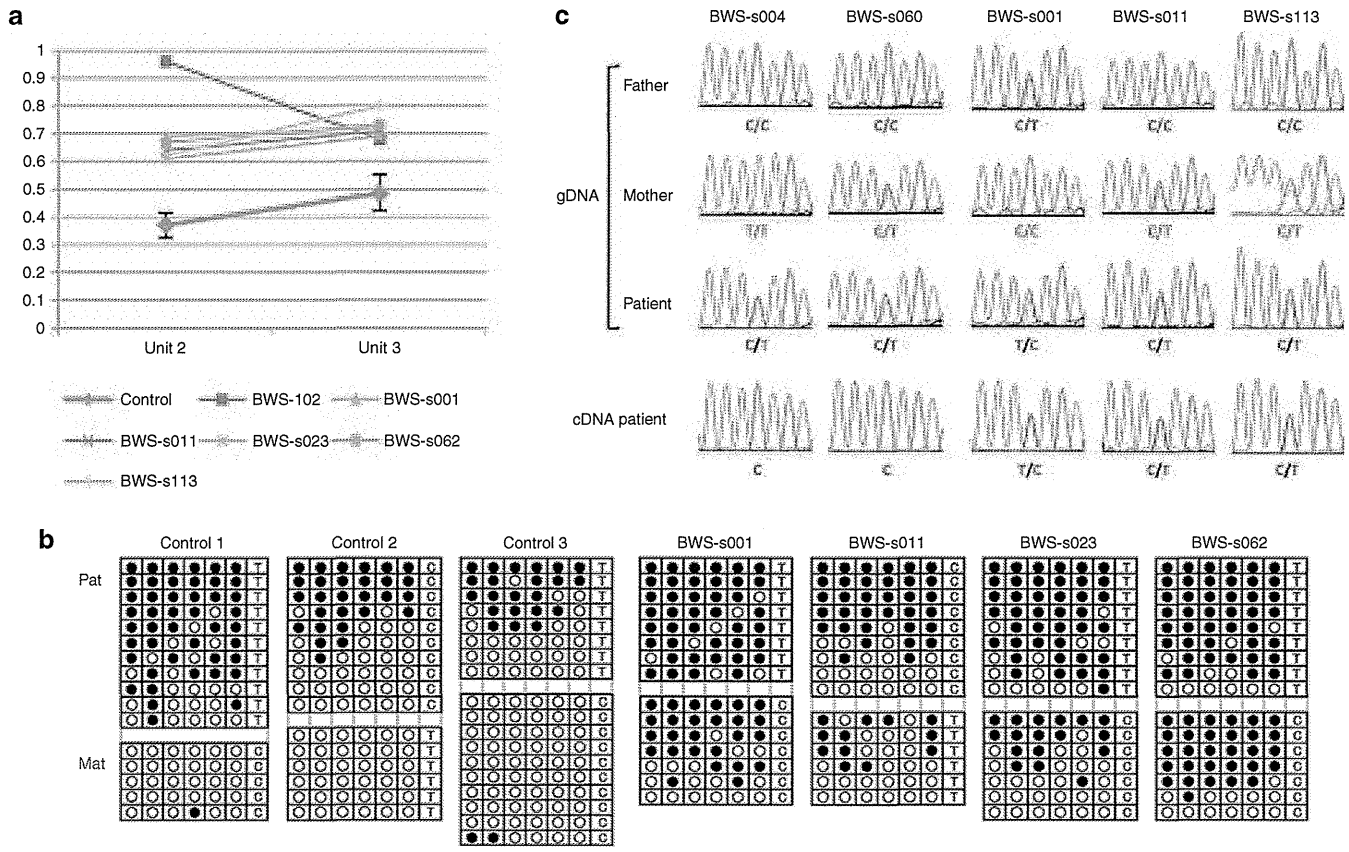

Figure 3 Methylation analysis of *ZDBF2*-DMR and expression analysis of the *ZDBF2* gene. (**a**) Results of matrix-assisted laser desorption/ionization mass spectrometry analysis. Averages with SD of 24 normal controls are shown in blue. Methylation indexes of the patients showing GOM are indicated in different colors. Units 1 and 2 included two and one CpG sites, respectively. (**b**) Results of bisulfite sequencing. Normal controls show monoallelic differential methylation, whereas four Beckwith–Wiedemann syndrome (BWS) patients (BWS-s001, BWS-s011, BWS-s023, and BWS-s060) show biallelic methylation. Two parental alleles were distinguished by a SNP (*rs1861437*). Mat, maternal allele; Pat, paternal allele. (**c**) Results of expression analysis of the *ZDBF2* gene. Three BWS patients (BWS-s001, BWS-s011, and BWS-s113) heterozygous for a coding SNP (*rs10932150*) with GOM clearly showed biallelic expression; by contrast, two patients with normally methylated differentially methylated region (DMRs) exhibited paternal monoallelic expression (patients BWS-s004 and BWS-s060). gDNA, genomic DNA; GOM, gain of methylation; SNP, single-nucleotide polymorphism.

which suggests that our definition of aberrant methylation is appropriate. In addition, we investigated the expression levels of *ZDBF2* and *FAM50B* by quantitative RT-PCR. The expression levels in patients with aberrantly methylated DMRs were higher than those in patients with normally methylated DMRs (**Supplementary Figure S6** online). These results indicate that allelic expression and expression levels were indeed associated with the methylation status of the corresponding DMR in patients with MMDs.

Lack of pathological variation in all aberrantly methylated DMRs in *Kv*DMR1-LOM patients

Because the genetic aberrations of *H19*DMR explained only ~20% of BWS patients with *H19*DMR-GOM,[28] we hypothesized the existence of *cis*-acting variations within aberrantly methylated DMRs. Therefore, we sequenced all aberrantly methylated DMRs, including *Kv*DMR1, in *Kv*DMR1-LOM patients. However, no variations were found in any aberrantly hypomethylated DMRs, except for four known SNPs (summarized in **Supplementary Figure S7** online), suggesting that *cis*-acting pathological variations are not involved in aberrant methylation of these DMRs.

No difference in clinical features between MMDs and monolocus methylation defects

In *Kv*DMR1-LOM patients, there was no significant difference in clinical features between MMDs and monolocus methylation defects, which demonstrated LOM only at *Kv*DMR1 (Table 1). Among 27 patients with *Kv*DMR1-LOM for whom information on conception was available, one patient was conceived using intracytoplasmic sperm injection, two were from artificial insemination by the husband, and two were from ovulation stimulation. We searched for a link between assisted reproductive technology and MMD but could find no relationship (Table 1). The average age of neither the mother nor the father differed between patients with MMDs versus those with monolocus methylation defects (Table 1). The fact that monozygotic twins discordant for BWS were found predominantly for females suggests an insufficient amount of DNA methyltransferase 1 (DNMT1) to maintain *Kv*DMR1 methylation during the overlap in timing

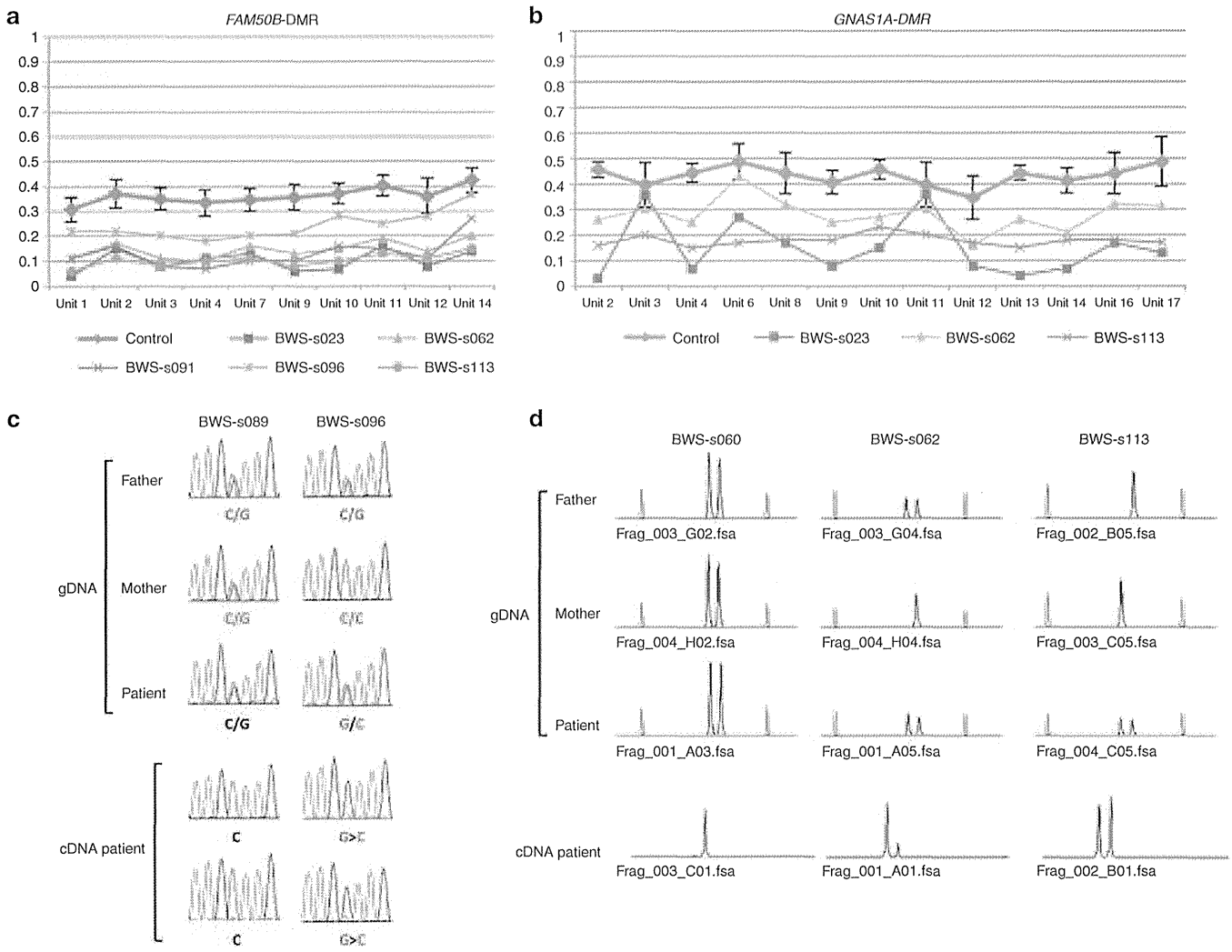

Figure 4 Methylation analysis of *FAM50B*- and *GNAS1A*-DMRs and expression analysis of the *FAM50B* and *GNAS1A* genes. (**a**,**b**) Results of matrix-assisted laser desorption/ionization mass spectrometry analysis. Averages with SD of 24 normal controls are shown in blue. Methylation indexes of patients showing LOM are indicated in different colors. Ten CpG units analyzed for *FAM50B*-DMR covered 13 CpG sites, and 13 CpG units analyzed for *GNAS1A*-DMR covered 18 CpG sites. (**c**) Results of expression analysis of the *FAM50B* gene. Beckwith–Wiedemann syndrome (BWS) patient BWS-s096 was heterozygous for a coding SNP (*rs6597007*) with LOM and showed biallelic expression with a low peak of maternal expression, whereas monoallelic expression was seen in a patient with normally methylated differentially methylated regions (DMRs) (patient BWS-s089). In patient BWS-s096, maternal expression was noted in two independent analyses despite low-grade LOM. gDNA, genomic DNA. (**d**) Results of expression analysis of the *GNAS1A* gene. Patients BWS-s062 and BWS-s113, heterozygous for a deletion/insertion variation (*rs143800311*) with LOM, showed biallelic expression, whereas patient BWS-s060 possessed normally methylated DMRs and exhibited monoallelic expression. Maternal expression was noted despite low-grade LOM in patient BWS-s062. Red peaks are molecular markers. GOM, gain of methylation; LOM, loss of methylation.

with X-chromosome inactivation and twinning.[29] This hypothesis suggests that females might tend to suffer from MMDs. We compared the frequency of female patients with MMDs with the frequency of those with monolocus methylation defects, but no significant difference could be found (Table 1).

DISCUSSION

Currently, most reports have studied 3–10 imprinted DMRs in BWS patients,[7–10,13] with the exception of two reports in which 16 and 27 DMRs were analyzed.[11,12] In addition, the quantitative capability of methods used for multiple methylation analyses has been variable, and few studies have conducted multiple checks to confirm the methylation statuses of all DMRs showing aberrant methylation.[7–13] To resolve these matters, we analyzed 29 DMRs and confirmed all aberrantly methylated DMRs using MALDI-TOF MS and bisulfite pyrosequencing, which are the most reliable quantitative methods of methylation analysis available at present.[19,30,31] We found that 34.1% of *Kv*DMR1-LOM patients exhibited MMDs. The frequency was higher than that in previous reports, which can be summarized as reporting an overall frequency of 20.6% (102 of 495 patients).[7–13] However, within these reports, the frequency in studies that analyzed 10 or fewer DMRs is 19.0% (82 of 431),[7–10,13] and the frequency in studies that analyzed more than 10 DMRs is 31.3% (20 of

Table 1 Clinical features of *Kv*DMR-LOM patients with monolocus methylation defect and those with multilocus methylation defects

	Methylation defect		
	Monolocus	**Multilocus**	***P* value**
Sex			0.22
Male	15	5	
Female	13	9	
Average age of patients	3.3	2.4	0.098[a]
Average age of parents			
Father	31.8	33.8	0.93[a]
Mother	31.8	30.3	0.37[a]
Assisted reproduction technology	3/19 (20%) (AIH 2, OS 1)	2/8 (29%) (ICSI 1, OS 1)	0.47
Standard deviation of average birth weight	+1.9	+2.0	0.58[a]
Overgrowth	21/28 (75%)	9/13 (69%)	0.78
Abdominal wall defect	22/29 (76%)	12/13 (92%)	0.21
Macroglossia	29/29 (100%)	12/12 (100%)	0.60
Hypoglycemia	14/27 (52%)	5/12 (42%)	0.41
Ear pits and creases	19/27 (70.4%)	8/12 (67%)	0.73
Nevus flammeus	9/26 (35%)	4/10 (40%)	0.53
Hemihypertrophy	6/27 (22%)	6/13 (46%)	0.12
Renal anomaly	2/26 (8%)	0/11 (0%)	0.49
Renal enlargement	6/28 (21%)	1/13 (8%)	0.27
Adrenal enlargement	1/27 (4%)	0/11 (0%)	0.71
Hepatomegaly	5/29 (17%)	2/12 (17%)	0.67
Splenomegaly	6/29 (21%)	2/12 (17%)	0.57
Abnormal external genitalia	2/28 (7%)	0/12 (0%)	0.49
Increased bone age	2/15 (13%)	0/3 (0%)	0.69
Cardiac anomaly	2/23 (9%)	0/11 (0%)	0.82
Developmental retardation	6/22 (27%)	0/9 (0%)	0.10
Childhood tumor	5/26 (19%)	0/11 (0%)	0.15

AIH, artificial insemination by husband; ICSI, intracytoplasmic sperm injection; LOM, loss of methylation; OS, ovulation stimulation.

[a]Mann–Whitney *U*-test. Fisher's exact test was used for other analyses.

64).[11,12] In addition, we found that 30.0% of *H19*DMR-GOM patients showed MMDs, which is surprising considering that no MMDs were found in two previous reports in which 10 and 16 DMRs were analyzed.[8,11] These data suggest that the greater the number of DMRs analyzed, the higher the frequency of MMDs observed. In future, all DMRs in the genome should be analyzed to understand the precise frequency of MMDs, which DMRs become preferentially aberrantly methylated, and the mechanism by which MMDs occur.

In both *Kv*DMR1-LOM patients and *H19*DMR-GOM patients, we found MMDs in which not only LOM but also GOM were seen. We also found that both matDMRs and patDMRs were aberrantly methylated in both patient groups. It is noteworthy that matDMRs, probably gametic maternally methylated DMRs, were more susceptible to aberrant methylation than patDMRs in *Kv*DMR1-LOM patients, although no particular parent-based pattern of aberrant methylation has been reported previously.[12] This suggests that gametic maternally methylated DMRs are vulnerable to DNA demethylation during the preimplantation stage of early embryogenesis when *Kv*DMR1-LOM occurs.

Although it has not been reported that aberrant methylation of the corresponding DMR affects imprinted gene expression in MMD patients, we found biallelic expression of three imprinted genes (*ZDBF2*, *FAM50B*, and *GNAS1A*) to be associated with the aberrant methylation of their respective DMRs. Because biallelic expression increased the total expression levels of *ZDBF2* and *FAM50B*, we expect that had we measured the expression levels of *GNAS1A*, we would have observed an increase. Therefore, alteration of gene expression levels due to MMDs might affect the phenotype; however, clinical features between MMDs and monolocus methylation defects were not different in our study. This lack of difference has been previously reported,[7,9,10,13] although a few groups have reported a

difference in clinical features.[8,11,12] Two reasons for this similarity in terms of clinical features could be suggested. First, the mosaic ratio might be different in each organ. Because aberrant methylation was generally partial, it would occur after fertilization, and the patients would be mosaic. A high mosaic ratio would be a critical factor in the emergence of a distinct phenotype in BWS patients with monolocus methylation defects. Second, the imprinted locus at 11p15 might be epidominant over other imprinted loci because all MMD patients were clinically diagnosed as BWS.

Regarding the causative factor(s) for MMD, we could not find any pathological variation in any aberrantly methylated DMR, including *Kv*DMR1, suggesting that *cis*-acting variations of each specific DMR itself were not involved in the genesis of MMDs. On the other hand, the involvement of *trans*-acting factors has been advocated in other reports because mutations of *ZFP57* (which are required for the postfertilization maintenance of maternal and paternal methylation imprinting at multiple loci) have been found in transient neonatal diabetes mellitus type 1 patients with multilocus hypomethylation.[32] Mutations of *NLRP2* were also identified in a BWS patient with *Kv*DMR1-LOM and *MEST*-LOM in a family with complex consanguinity and in a Silver–Russell syndrome patient with multilocus hypomethylation.[12,33] In addition, TRIM28, NLRP7, KHDC3L, and DNMT3L have been considered to be candidate *trans*-acting factors. However, no mutations in any of these candidates or other genes, such as *DNMT1*, *DNMT3A*, and *DNMT3B*, were found in our BWS patients with MMDs, as determined by exome sequencing (K. Sasaki and K. Hata, personal communication). Recently, Lorthongpanich et al.[34] reported that the absence of maternal *Trim28* until zygotic gene activation at the two-cell late stage caused mosaicism of MMDs randomly, suggesting that insufficient expression of the candidate gene(s) at very early embryogenesis is an important event in the generation of MMDs in human imprinted diseases. Whole-genome sequencing and whole-genome bisulfite sequencing, including the regulatory regions of the candidate genes, and transcriptome analysis in early embryogenesis would be useful to identify the cause(s) of MMDs.

In our *H19*DMR-GOM patients, we also found GOM of *IGF2*-DMR0 and *IGF2*-DMR2 to be associated with GOM of *H19*DMR and *H19promoter* DMR, in agreement with previous reports.[22,35,36] Two patients showed simultaneous GOM at both *IGF2*-DMRs. Because *Igf2*-DMRs were established at the postimplantation stage under the control of *H19*DMR in mice,[37] GOM of *IGF2*-DMRs in BWS is likely to occur at the same stage. Although the function of *IGF2*-DMR0 is still unknown, methylated *Igf2*-DMR2 plays a role in transcription initiation of *Igf2* in mice.[38] GOM of the DMRs might change the high-order chromatin structure of the maternal allele and increase the expression of *IGF2* in cooperation with *H19*DMR-GOM in BWS patients.

In conclusion, our comprehensive and quantitative methylation analysis of multiple imprinted DMRs revealed several new findings: (i) matDMRs, probably gametic maternally methylated DMRs, are more susceptible to aberrant methylation during the preimplantation stage, when *Kv*DMR1-LOM occurs; (ii) aberrant methylation indeed alters imprinted gene expression; and (iii) *cis*-acting pathological variations of each DMR are not involved in the MMDs analyzed. Moreover, our study confirmed the simultaneous aberrant hypermethylation of *IGF2*-DMR0 and/or -DMR2 with isolated *H19*DMR-GOM. These findings may help us to understand the molecular mechanisms and pathophysiological features of MMDs.

SUPPLEMENTARY MATERIAL

Supplementary material is linked in the online version of the paper at http://www.nature.com/gim.

ACKNOWLEDGMENTS

We thank all the participants and their families who provided samples and all the doctors who referred patients to us. This study was supported, in part, by a Grant for Research on Intractable Diseases from the Ministry of Health, Labor, and Welfare; a Grant for Child Health and Development from the National Center for Child Health and Development; a Grant-in-Aid for Challenging Exploratory Research; and a Grant-in-Aid for Scientific Research (C) from the Japan Society for the Promotion of Science.

DISCLOSURE

The authors declare no conflict of interest.

REFERENCES

1. Abramowitz LK, Bartolomei MS. Genomic imprinting: recognition and marking of imprinted loci. *Curr Opin Genet Dev* 2012;22:72–78.
2. Tomizawa S, Sasaki H. Genomic imprinting and its relevance to congenital disease, infertility, molar pregnancy and induced pluripotent stem cell. *J Hum Genet* 2012;57:84–91.
3. Weksberg R, Shuman C, Beckwith JB. Beckwith-Wiedemann syndrome. *Eur J Hum Genet* 2010;18:8–14.
4. Choufani S, Shuman C, Weksberg R. Beckwith-Wiedemann syndrome. *Am J Med Genet C Semin Med Genet* 2010;154C:343–354.
5. Soejima H, Higashimoto K. Epigenetic and genetic alterations of the imprinting disorder Beckwith-Wiedemann syndrome and related disorders. *J Hum Genet* 2013;58:402–409.
6. Mackay DJ, Boonen SE, Clayton-Smith J, et al. A maternal hypomethylation syndrome presenting as transient neonatal diabetes mellitus. *Hum Genet* 2006;120:262–269.
7. Rossignol S, Steunou V, Chalas C, et al. The epigenetic imprinting defect of patients with Beckwith-Wiedemann syndrome born after assisted reproductive technology is not restricted to the 11p15 region. *J Med Genet* 2006;43:902–907.
8. Bliek J, Verde G, Callaway J, et al. Hypomethylation at multiple maternally methylated imprinted regions including PLAGL1 and GNAS loci in Beckwith-Wiedemann syndrome. *Eur J Hum Genet* 2009;17:611–619.
9. Azzi S, Rossignol S, Steunou V, et al. Multilocus methylation analysis in a large cohort of 11p15-related foetal growth disorders (Russell Silver and Beckwith Wiedemann syndromes) reveals simultaneous loss of methylation at paternal and maternal imprinted loci. *Hum Mol Genet* 2009;18:4724–4733.
10. Lim D, Bowdin SC, Tee L, et al. Clinical and molecular genetic features of Beckwith-Wiedemann syndrome associated with assisted reproductive technologies. *Hum Reprod* 2009;24:741–747.
11. Poole RL, Docherty LE, Al Sayegh A, et al.; International Clinical Imprinting Consortium. Targeted methylation testing of a patient cohort broadens the epigenetic and clinical description of imprinting disorders. *Am J Med Genet A* 2013;161:2174–2182.
12. Court F, Martin-Trujillo A, Romanelli V, et al. Genome-wide allelic methylation analysis reveals disease-specific susceptibility to multiple methylation defects in imprinting syndromes. *Hum Mutat* 2013;34:595–602.

13. Tee L, Lim DH, Dias RP, et al. Epimutation profiling in Beckwith-Wiedemann syndrome: relationship with assisted reproductive technology. *Clin Epigenetics* 2013;5:23.
14. DeBaun MR, Tucker MA. Risk of cancer during the first four years of life in children from The Beckwith-Wiedemann Syndrome Registry. *J Pediatr* 1998;132(3 Pt 1):398–400.
15. Soejima H, Nakagawachi T, Zhao W, et al. Silencing of imprinted CDKN1C gene expression is associated with loss of CpG and histone H3 lysine 9 methylation at DMR-LIT1 in esophageal cancer. *Oncogene* 2004;23:4380–4388.
16. Higashimoto K, Nakabayashi K, Yatsuki H, et al. Aberrant methylation of H19-DMR acquired after implantation was dissimilar in soma versus placenta of patients with Beckwith-Wiedemann syndrome. *Am J Med Genet A* 2012;158A:1670–1675.
17. Yatsuki H, Higashimoto K, Jozaki K, et al. Novel mutations of CDKN1C in Japanese patients with Beckwith-Wiedemann syndrome. *Genes & Genomics* 2013;35:141–147.
18. Higashimoto K, Jozaki K, Kosho T, et al. A novel de novo point mutation of the OCT-binding site in the IGF2/H19-imprinting control region in a Beckwith-Wiedemann syndrome patient. *Clin Genet* 2013; e-pub ahead of print 8 November 2013.
19. Ehrich M, Nelson MR, Stanssens P, et al. Quantitative high-throughput analysis of DNA methylation patterns by base-specific cleavage and mass spectrometry. *Proc Natl Acad Sci USA* 2005;102:15785–15790.
20. Rumbajan JM, Maeda T, Souzaki R, et al. Comprehensive analyses of imprinted differentially methylated regions reveal epigenetic and genetic characteristics in hepatoblastoma. *BMC Cancer* 2013;13:608.
21. Cui H, Onyango P, Brandenburg S, Wu Y, Hsieh CL, Feinberg AP. Loss of imprinting in colorectal cancer linked to hypomethylation of H19 and IGF2. *Cancer Res* 2002;62:6442–6446.
22. Murrell A, Ito Y, Verde G, et al. Distinct methylation changes at the IGF2-H19 locus in congenital growth disorders and cancer. *PLoS One* 2008;3: e1849.
23. Woodfine K, Huddleston JE, Murrell A. Quantitative analysis of DNA methylation at all human imprinted regions reveals preservation of epigenetic stability in adult somatic tissue. *Epigenetics Chromatin* 2011;4:1.
24. Reik W, Maher ER. Imprinting in clusters: lessons from Beckwith-Wiedemann syndrome. *Trends Genet* 1997;13:330–334.
25. Kobayashi H, Yamada K, Morita S, et al. Identification of the mouse paternally expressed imprinted gene Zdbf2 on chromosome 1 and its imprinted human homolog ZDBF2 on chromosome 2. *Genomics* 2009;93:461–472.
26. Nakabayashi K, Trujillo AM, Tayama C, et al. Methylation screening of reciprocal genome-wide UPDs identifies novel human-specific imprinted genes. *Hum Mol Genet* 2011;20:3188–3197.
27. Liu J, Litman D, Rosenberg MJ, Yu S, Biesecker LG, Weinstein LS. A GNAS1 imprinting defect in pseudohypoparathyroidism type IB. *J Clin Invest* 2000;106:1167–1174.
28. Demars J, Shmela ME, Rossignol S, et al. Analysis of the IGF2/H19 imprinting control region uncovers new genetic defects, including mutations of OCT-binding sequences, in patients with 11p15 fetal growth disorders. *Hum Mol Genet* 2010;19:803–814.
29. Weksberg R, Shuman C, Caluseriu O, et al. Discordant KCNQ1OT1 imprinting in sets of monozygotic twins discordant for Beckwith-Wiedemann syndrome. *Hum Mol Genet* 2002;11:1317–1325.
30. Tost J, Dunker J, Gut IG. Analysis and quantification of multiple methylation variable positions in CpG islands by Pyrosequencing. *Biotechniques* 2003;35:152–156.
31. Claus R, Wilop S, Hielscher T, et al. A systematic comparison of quantitative high-resolution DNA methylation analysis and methylation-specific PCR. *Epigenetics* 2012;7:772–780.
32. Mackay DJ, Callaway JL, Marks SM, et al. Hypomethylation of multiple imprinted loci in individuals with transient neonatal diabetes is associated with mutations in ZFP57. *Nat Genet* 2008;40:949–951.
33. Meyer E, Lim D, Pasha S, et al. Germline mutation in NLRP2 (NALP2) in a familial imprinting disorder (Beckwith-Wiedemann Syndrome). *PLoS Genet* 2009;5:e1000423.
34. Lorthongpanich C, Cheow LF, Balu S, et al. Single-cell DNA-methylation analysis reveals epigenetic chimerism in preimplantation embryos. *Science* 2013;341:1110–1112.
35. Reik W, Brown KW, Schneid H, Le Bouc Y, Bickmore W, Maher ER. Imprinting mutations in the Beckwith-Wiedemann syndrome suggested by altered imprinting pattern in the IGF2-H19 domain. *Hum Mol Genet* 1995;4:2379–2385.
36. Sparago A, Russo S, Cerrato F, et al. Mechanisms causing imprinting defects in familial Beckwith-Wiedemann syndrome with Wilms' tumour. *Hum Mol Genet* 2007;16:254–264.
37. Lopes S, Lewis A, Hajkova P, et al. Epigenetic modifications in an imprinting cluster are controlled by a hierarchy of DMRs suggesting long-range chromatin interactions. *Hum Mol Genet* 2003;12:295–305.
38. Murrell A, Heeson S, Bowden L, et al. An intragenic methylated region in the imprinted Igf2 gene augments transcription. *EMBO Rep* 2001;2:1101–1106.

Journal of Human Genetics (2014), 1–5

www.nature.com/jhg

SHORT COMMUNICATION

Silver–Russell syndrome without body asymmetry in three patients with duplications of maternally derived chromosome 11p15 involving *CDKN1C*

Shinichi Nakashima[1], Fumiko Kato[1], Tomoki Kosho[2], Keisuke Nagasaki[3], Toru Kikuchi[4], Masayo Kagami[5], Maki Fukami[5] and Tsutomu Ogata[1]

We report duplications of maternally derived chromosome 11p15 involving *CDKN1C* encoding a negative regulator for cell proliferation in three Japanese patients (cases 1 and 2 from family A and case 3 from family B) with Silver–Russell syndrome (SRS) phenotype lacking hemihypotrophy. Chromosome analysis showed 46,XX,der(16)t(11;16)(p15.3;q24.3)mat in case 1, 46, XY,der(16)t(11;16)(p15.3;q24.3)mat in case 2 and a *de novo* 46,XX,der(17)t(11;17)(p15.4;q25.3) in case 3. Genomewide oligonucleotide-based array comparative genomic hybridization, microsatellite analysis, pyrosequencing-based methylation analysis and direct sequence analysis revealed the presence of maternally derived extra copies of the distal chromosome 11p involving the wild-type *CDKN1C* (a ~7.98 Mb region in cases 1 and 2 and a ~4.43 Mb region in case 3). The results, in conjunction with the previous findings in patients with similar duplications encompassing *CDKN1C* and in those with intragenic mutations of *CDKN1C*, imply that duplications of *CDKN1C*, as well as relatively mild gain-of-function mutations of *CDKN1C* lead to SRS subtype that usually lack hemihypotrophy.
Journal of Human Genetics (2014) **00**, 1–5. doi:10.1038/jhg.2014.100

INTRODUCTION

Silver–Russell syndrome (SRS) is a congenital developmental disorder characterized by pre- and postnatal growth failure, relative macrocephaly, hemihypotrophy and fifth-finger clinodactyly.[1] Recent studies have shown that epimutation (hypomethylation) of the paternally derived *H19*-differentially methylated region (DMR) at the imprinting control region 1 (ICR1) on chromosome 11p15.5 and maternal uniparental disomy 7 account for ~45 and ~5% of SRS patients, respectively.[1] Thus, underlying (epi)genetic factors still remain to be clarified in a substantial fraction of SRS patients, although several rare (epi)genetic aberrations have been identified in a small fraction of SRS patients.[1]

CDKN1C (cyclin-dependent kinase inhibitor 1C) is a maternally expressed gene that resides at the ICR2 just proximal to the ICR1.[2] *CDKN1C* encodes a negative regulator for cell proliferation and, consistent with this, loss-of-function mutations of *CDKN1C* cause Beckwith–Wiedemann syndrome associated with overgrowth.[2,3] Furthermore, recent studies have shown that gain-of-function mutations of *CDKN1C* result in IMAGe syndrome (IMAGeS) characterized by intrauterine growth restriction, metaphyseal dysplasia, adrenal hypoplasia congenita and male genital abnormalities,[2] whereas less severe gain-of-function mutations of *CDKN1C* have been identified in a large family with maternally inherited SRS.[4] Thus, it has been suggested that relatively severe and mild *CDKN1C* gain-of-function effects lead to IMAGeS and SRS, respectively.[4,5] Notably, IMAGeS patients satisfy the diagnostic criteria for SRS proposed by Nechine *et al.*[5,6] and IMAGeS and SRS patients with *CDKN1C* mutations invariably lack hemihypotrophy characteristic of SRS.[4–6]

Here, we report three patients with SRS and duplications of maternally derived chromosome 11p15.5 involving *CDKN1C*. The results, in conjunction with previous findings, imply that duplications of *CDKN1C*, as well as relatively mild gain-of-function mutations of *CDKN1C* lead to SRS subtype that usually lack hemihypotrophy.

CASE REPORTS

Patients

We studied three Japanese patients (cases 1–3) from two families (Figure 1). Cases 1–3 satisfied the SRS diagnostic criteria proposed by Netchine *et al.*,[6] although they lacked hemihypotrophy (Table 1, see its footnote for Netchine SRS criteria). Oligohydramnios characteristic of SRS[7] was also noticed during the pregnancies of cases 2 and 3. They exhibited no IMAGeS-like phenotypes such as radiologically discernible skeletal dysplasia, an episode suggestive of adrenal dysfunction or undermasculinized genitalia in male case 2.

[1]Department of Pediatrics, Hamamatsu University School of Medicine, Hamamatsu, Japan; [2]Department of Human Genetics, Shinshu University School of Medicine, Matsumoto, Japan; [3]Department of Pediatrics, Niigata University School of Medicine, Niigata, Japan; [4]Department of Pediatrics, Saitama Medical University, Saitama, Japan and [5]Department of Molecular Endocrinology, National Research Institute for Child Health and Development, Tokyo, Japan
Correspondence: Professor T Ogata, Department of Pediatrics, Hamamatsu University School of Medicine, 1-20-1, Handayama, Higashi-ku, Hamamatsu, Shizuoka 431-3192, Japan.
E-mail: tomogata@hama-med.ac.jp
Received 10 October 2014; revised 28 October 2014; accepted 31 October 2014

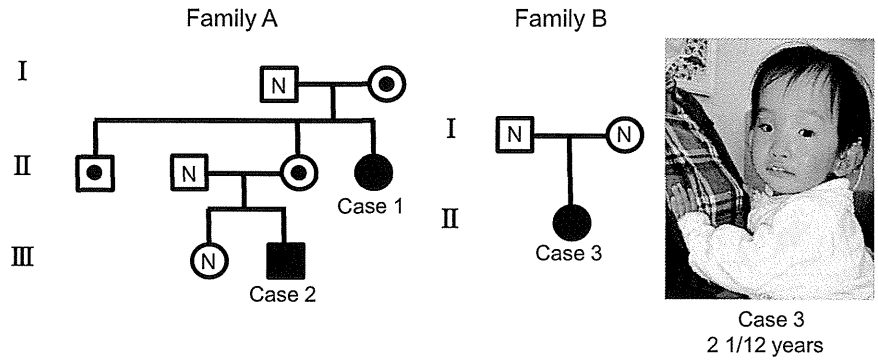

Figure 1 The pedigrees of families A and B and a photograph of case 3. In family A, cases 1 and 2 have an unbalanced translocation involving the distal part of chromosome 11p, the mothers of cases 1 and 2, as well as the brother of case 1 have a balanced translocation involving the distal part of chromosome 11p and the remaining subjects have a normal karyotype. In family B, case 3 has an unbalanced translocation involving the distal part of chromosome 11p and the parents have a normal karyotype. Case 3 exhibits SRS-compatible phenotypes such as prominent forehead, triangular face with relative macrocephaly and micrognathia, ear anomalies and short and curved fifth fingers, but is free from hemihypotrophy.

Table 1 Clinical features of cases 1–3 and reported cases with duplications of maternally derived chromosome 11p15 involving *CDKN1C*

	Case 1 family A female	*Case 2 family A male*	*Case 3 family B female*	*Reported cases (n = 16)*[11–19]
SRS phenotype				
Mandatory criteria for SRS				
BL and/or BW ⩽ −2 SDS	+	+	+	16/16
Scoring system criteria for SRS				
Relative macrocephaly at birth[a]	Unknown	+	+	11/11
PH ⩽ −2 SDS at ⩾2 years	+	Unknown	+	14/14
Prominent forehead	+	+	+	8/9
Body asymmetry	−	−	−	1/15
Feeding difficulties	+	−	Unknown	6/6
Other findings				
Gestational age (weeks)	39	32	32	22–38
Oligohydramnios	Unknown	+	+	Unknown
BL, cm (SDS)	38.0 (−4.9)	34.0 (−3.3)	32.0 (−3.9)	N.D.[b]
BW, kg (SDS)	1.3 (−5.3)	0.87 (−3.6)	0.82 (−3.7)	N.D.[b]
BOFC, cm (SDS)	29.5 (−2.7)	28.3 (−0.6)	27 (−1.2)	N.D.[b]
Present age (years:months)	14:00	1:03	3:03	1–31
PH, cm (SDS)	130.7 (−4.7)	60.8 (−6.4)	70.7 (−6.7)	N.D.[b]
PW, kg (SDS)	37.5 (−1.2)	4.8 (−5.3)	6.8 (−4.0)	N.D.[b]
BMI, kg m^{-2} (SDS)	22.0 (0.7)	13.1 (−2.8)	13.6 (−1.5)	N.D.[b]
POFC, cm (SDS)	Unknown	45.0 (−0.5)	48.5 (−0.1)	N.D.[b]
Relative macrocephaly at present[c]	Unknown	+	+	14/15
Triangular face	−	+	+	12/16
Ear anomalies	−	−	+	8/11
Irregular teeth	Unknown	+	+	1/2
Clinodactyly	+	+	+	10/11
Brachydactyly	+	+	−	4/5
Simian crease	+	+	−	1/2
Muscular hypotonia	Unknown	+	+	4/7
Developmental/speech delay	+	+	+	11/15
IMAGe syndrome phenotype				
IUGR	+	+	+	16/16
Metaphyseal dysplasia	−	−	−	Not described
Adrenal hypoplasia	−	−[d]	−[e]	Not described
Genital abnormality	Female	−	Female	Not described

The diagnosis of Silver–Russell syndrome is made when a patient is positive for the mandatory criteria and at least three of the five scoring system criteria (Netchine *et al.*[5])
Abbreviations: BL, birth length; BMI, body mass index; BOFC, birth occipitofrontal circumference; BW, birth weight; IMAGe, intrauterine growth restriction, metaphyseal dysplasia, adrenal hypoplasia congenita and male genital abnormalities; IUGR, intrauterine growth retardation; N.D., not determined; PH, present height; POFC, present occipitofrontal circumference; PW, present weight; SDS, standard deviation score.
For reported cases, the denominators indicate the number of patients examined for the presence or absence of each feature, and the numerators represent the number of patients assessed to be positive for that feature.
Birth and present body sizes were assessed by the gestational/postnatal age- and sex-matched Japanese reference data from the Ministry of Health, Labor and Welfare and from the Ministry of Education, Science, Sports and Culture.
[a]BL or BW (SDS)—BOFC (SDS) ⩽ −1.5.
[b]N.D. because of various ethnicities of affected individuals and descriptions of height assessment (percentile and SDS).
[c]PH or PW (SDS)—POFC (SDS) ⩽ −1.5.
[d]A rapid adrenocorticotropin stimulation test (0.25 mg m^{-2} bolus i.v.; blood sampling at 0 and 60 min) showed a sufficient cortisol response (14.2 → 26.2 μg dl^{-1}) (reference range >20 μg dl^{-1}).
[e]A growth hormone releasing peptide 2 stimulation test (2 μg kg^{-1} bolus i.v.; blood sampling at 0, 15, 30, 45 and 60 min) yielded a sufficient cortisol response (18.4 → 25.5 μg dl^{-1}).

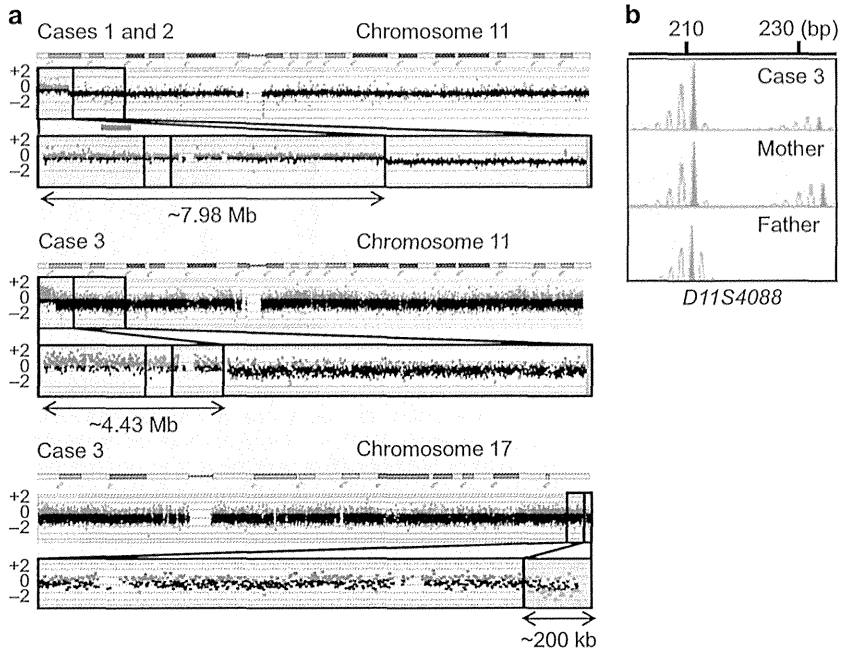

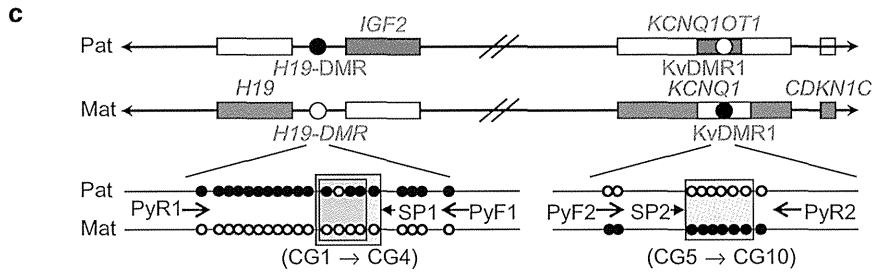

	Case 1			Case 2			Case 3			Controls (n=50)
	P	F	M	P	F	M	P	F	M	Median (Range)
CG1	30	41	53	34	52	55	29	44	44	45 (36 ~ 55)
CG2	31	42	54	37	54	55	28	43	44	46 (36 ~ 57)
CG3	33	45	56	38	57	60	31	47	46	50 (39 ~ 64)
CG4	33	44	55	39	56	57	31	48	46	48 (37 ~ 60)
CG5	72	56	56	72	56	57	68	56	57	58 (49 ~ 66)
CG6	78	59	59	73	59	60	71	61	58	61 (52 ~ 68)
CG7	67	52	50	66	50	52	61	50	49	48 (41 ~ 54)
CG8	69	55	53	68	53	55	63	52	52	48 (42 ~ 55)
CG9	78	60	61	75	63	61	72	63	59	67 (55 ~ 72)
CG10	74	63	57	79	60	59	77	63	64	64 (55 ~ 71)

Figure 2 Representative molecular findings. (**a**) Array comparative genomic hybridization analysis. The black, red and green dots represent signals indicative of the normal, increased (log2 signal ratio > +0.5) and decreased (log2 signal ratio < −0.8) copy numbers, respectively. The log2 signal ratios of +0.5 and −1.0 indicate the presence of three copies and a single copy of the corresponding regions, respectively. The red and the green rectangles represent increased and decreased copy number regions, respectively. The yellow rectangles denote the regions encompassing the ICR1 and the ICR2. (**b**) Microsatellite analysis for *D11S4088* proximal to the KvDMR1. Unequal amplification of the heterozygous peaks in each subject is consistent with short products being more easily amplified than long products and comparison of area under curves of the 212 bp and the 234 bp alleles between case 3 and the mother indicates the presence of two 212 bp alleles and a single 234 bp allele in case 3. This implies that the maternal 212 and 234 bp alleles and the paternal 212 bp allele have been transmitted to case 3. (**c**) Pyrosequencing-based methylation analysis of the *H19*-DMR at the ICR1 and the KvDMR1 at the ICR2, using bisulfite-treated genomic DNA. The cytosine residues at the CpG dinucleotides within the *H19*-DMR is methylated after paternal transmission (filled circles) and unmethylated after maternal transmission (open circles), whereas those within the KvDMR1 is unmethylated after paternal transmission (open circles) and methylated after maternal transmission (filled circles). Paternally and maternally expressed genes are shown in blue and red, respectively. For the *H19*-DMR, a segment encompassing 21 CpG dinucleotides was PCR amplified with PyF1 and PyR1 primers and a sequence primer (SP1) was hybridized to a single-stranded PCR product. Subsequently, the MIs were obtained for four CpG dinucleotides (CG1–CG4) (indicated with a yellow rectangle). The blue rectangle indicates the CTCF binding site 6. The CpG dinucleotide between CG1 and CG2 was not examined, because it constitutes a C/T SNP (indicated with gray circles). The KvDMR1 was similarly examined using PyF2 and PyR2 primers and SP2 and the MIs were obtained for CG5–CG10. The MIs are summarized in the bottom table. F, father; and M, mother; P, patient.

Cytogenetic and molecular studies

This study was approved by the Institute Review Board Committee at Hamamatsu University School of Medicine and was performed using peripheral leukocyte samples and primers shown in Supplementary Table S1 after obtaining written informed consent. The methods for molecular studies were as reported previously.[7] We also obtained written informed consent to publish the facial photograph of case 3 from the parents.

Chromosome analysis showed 46,XX,der(16)t(11;16)(p15.3;q24.3)mat in case 1, 46,XY,der(16)t(11;16)(p15.3;q24.3)mat in case 2 and a *de novo* 46,XX, der(17)t(11;17)(p15.4;q25.3) in case 3 (Figure 1). Then, genomewide oligonucleotide-based array comparative genomic hybridization was carried out using a catalog human array (2 × 400 K format, ID G4448A) (Agilent Technologies), revealing the presence of three copies of the distal parts of chromosome 11p involving the ICR1 and the ICR2 in cases 1–3 (a ~ 7.98 Mb region in cases 1 and 2 and a ~ 4.43 Mb region in case 3) (Figure 2a). No discernible deletion was identified on the distal chromosome 16q in cases 1 and 2, indicating the position of the chromosome 16q breakpoint at the very telomeric portion, whereas a ~ 200 kb deletion was detected in the telomeric portion of chromosome 17q in case 3. There was no other copy number alteration that was not registered in the Database of Genomic Variants (http://dgv.tcag.ca/dgv/app/home). Microsatellite analysis was carried out for four loci on the duplicated chromosome 11p, showing the presence of two alleles of maternal origin and a single allele of paternal origin in cases 1–3 (Figure 2b and Supplementary Table S2). Subsequently, pyrosequencing-based methylation analysis was performed for four CpG dinucleotides (CG1–CG4) within the *H19*-DMR and six CpG dinucleotides (CG5–CG10) within the KvDMR1 using bisulfite-treated leukocyte genomic DNA samples and methylation index (MI, the ratio of methylated clones) was obtained for each of CG1–CG10 using PyroMark Q24 (Qiagen) (Figure 2c). In cases 1–3, the MIs for CG1–CG4 were mildly decreased or around the lower limit of the normal range and those for CG5–CG10 were mildly increased or around the upper limit of the normal range. Direct sequence analysis showed no discernible mutation on the *CDKN1C* coding region.

DISCUSSION

Cases 1–3 had SRS without hemihypotrophy (body asymmetry) in the presence of maternally derived extra copies of the distal chromosome 11p involving the ICR1 and the ICR2. This implies that the SRS phenotype lacking hemihypotrophy in cases 1–3 is primarily caused by two copies of maternally expressed genes on the two ICRs. In this regard, of duplicated maternally expressed genes, *CDKN1C* functions as a negative growth regulator[8] and *CDKN1C* gain-of-function mutations have been identified in SRS and IMAGeS,[2,4,5] whereas neither *H19* nor *KCNQ1* appears to have a positive role in growth regulation. Indeed, *H19* is regarded as a possible tumor suppressor gene[9] and *KCNQ1* encoding a voltage-gated potassium channel is involved in cardiac arrhythmias.[10] Thus, it is likely that SRS phenotype lacking hemihypotrophy in cases 1–3 is primarily caused by the presence of two functional copies of the wild-type *CDKN1C*. It should be pointed out, however, that although the der(16)t(11;16)(p15.3;q24.3) chromosome in cases 1 and 2 had no discernible chromosome 16q deletion, the der(17)t(11;17)(p15.4;q25.3) chromosome in case 3 was missing the ~ 200 kb telomeric 17q region that harbors several genes. In addition, there are multiple nonimprinted genes on the duplicated chromosome 11p15 regions. Thus, altered dosage of such genes may have exerted a certain effect on growth patterns of cases 1–3.

An extra copy of maternally derived chromosome 11p15 involving *CDKN1C* has been identified in 16 patients (Table 1) (for detailed clinical features of each case, see Supplementary Table S3).[11–19] Notably, although they frequently show SRS-like phenotype, hemihypotrophy (body asymmetry) has been found only in a single case[12] and none of them exhibit IMAGeS-like skeletal, adrenal or genital manifestation. This provides further support for the notion that two copies of maternally derived *CDKN1C*, as well as mild gain-of-function mutations of *CDKN1C* usually lead to SRS subtype lacking hemihypotrophy.

CONFLICT OF INTEREST

The authors declare no conflict of interest.

ACKNOWLEDGEMENTS

This work was supported by Grants-in-Aid for Scientific Research (A) (25253023) and Research (B) (23390083) from the Japan Society for the Promotion of Science, by Grants for Research on Intractable Diseases (H22-161) from the Ministry of Health, Labor and Welfare (MHLW) and by Grant for National Center for Child Health and Development (25-10).

1 Eggermann, T. Russell-Silver syndrome. *Am. J. Med. Genet. C Semin. Med. Genet.* **154C**, 355–364 (2010).
2 Arboleda, V.A., Lee, H., Parnaik, R., Fleming, A., Banerjee, A. & Ferraz-de-Souza, B. *et al.* Mutations in the PCNA-binding domain of CDKN1C cause IMAGe syndrome. *Nat. Genet.* **44**, 788–792 (2012).
3 Soejima, H. & Higashimoto, K. Epigenetic and genetic alterations of the imprinting disorder Beckwith–Wiedemann syndrome and related disorders. *J. Hum. Genet.* **58**, 402–409 (2013).
4 Brioude, F., Oliver-Petit, I., Blaise, A., Praz, F., Rossignol, S. & Le Jule, M. *et al.* CDKN1C mutation affecting the PCNA-binding domain as a cause of familial Russell Silver syndrome. *J. Med. Genet.* **50**, 823–830 (2013).
5 Kato, F., Hamajima, T., Hasegawa, T., Amano, N., Horikawa, R. & Nishimura, G. *et al.* IMAGe syndrome: clinical and genetic implications based on investigations in three Japanese patients. *Clin. Endocrinol.* **80**, 706–713 (2014).
6 Netchine, I., Rossignol, S., Dufourg, M. N., Azzi, S., Rousseau, A. & Perin, L. *et al.* 11p15 imprinting center region 1 loss of methylation is a common and specific cause of typical Russell-Silver syndrome: clinical scoring system and epigenetic-phenotypic correlations. *J. Clin. Endocrinol. Metab.* **92**, 3148–3154 (2007).
7 Fuke, T., Mizuno, S., Nagai, T., Hasegawa, T., Horikawa, R. & Miyoshi, Y. *et al.* Molecular and clinical studies in 138 Japanese patients with Silver–Russell syndrome. *PLoS ONE* **8**, e60105 (2013).
8 Lee, M. H., Reynisdottir, I. & Massague, J. Cloning of p57(KIP2), a cyclin-dependent kinase inhibitor with unique domain structure and tissue distribution. *Genes Dev.* **9**, 639–649 (1995).
9 Hao, Y., Crenshaw, T., Moulton, T., Newcomb, E. & Tycko, B. Tumour-suppressor activity of H19 RNA. *Nature* **365**, 764–767 (1993).
10 Wang, Q., Curran, M. E., Splawski, I., Burn, T. C., Millholland, J. M. & VanRaay, T. J. *et al.* Positional cloning of a novel potassium channel gene: KVLQT1 mutations cause cardiac arrhythmias. *Nat. Genet.* **12**, 17–23 (1996).
11 Fisher, A. M., Thomas, N. S., Cockwell, A., Stecko, O., Kerr, B. & Temple, I. K. *et al.* Duplications of chromosome 11p15 of maternal origin result in a phenotype that includes growth retardation. *Hum. Genet.* **111**, 290–296 (2002).
12 Eggermann, T., Meyer, E., Obermann, C., Heil, I., Schüler, H. & Ranke, M. B. *et al.* Is maternal duplication of 11p15 associated with Silver–Russell syndrome? *J. Med. Genet.* **42**, e26 (2005).
13 Schönherr, N., Meyer, E., Roos, A., Schmidt, A., Wollmann, H. A. & Eggermann, T. *et al.* The centromeric 11p15 imprinting centre is also involved in Silver–Russell syndrome. *J. Med. Genet.* **44**, 59–63 (2007).
14 South, S. T., Whitby, H., Maxwell, T., Aston, E., Brothman, A. R. & Carey, J. C. Co-occurrence of 4p16.3 deletions with both paternal and maternal duplications of 11p15: modification of the Wolf–Hirschhorn syndrome phenotype by genetic alterations predicted to result in either a Beckwith–Wiedemann or Russell–Silver phenotype. *Am. J. Med. Genet. A* **146A**, 2691–2697 (2008).
15 Bliek, J., Snijder, S., Maas, S. M., Polstra, A., van der Lip, K. & Alders, M. *et al.* Phenotypic discordance upon paternal or maternal transmission of duplications of the 11p15 imprinted regions. *Eur. J. Med. Genet.* **52**, 404–408 (2009).

16 Eggermann, T., Spengler, S., Bachmann, N., Baudis, M., Mau-Holzmann, U. A. & Singer, S. *et al.* Chromosome 11p15 duplication in Silver-Russell syndrome due to a maternally inherited translocation t(11;15). *Am. J. Med. Genet. A* **152A**, 1484–1487 (2010).
17 Cardarelli, L., Sparago, A., De Crescenzo, A., Nalesso, E., Zavan, B. & Cubellis, M. V. *et al.* Silver-Russell syndrome and Beckwith–Wiedemann syndrome phenotypes associated with 11p duplication in a single family. *Pediatr. Dev. Pathol.* **13**, 326–330 (2010).
18 Bonaldi, A., Mazzeu, J. F., Costa, S. S., Honjo, R. S., Bertola, D. R. & Albano, L. M. *et al.* Microduplication of the ICR2 domain at chromosome 11p15 and familial Silver-Russell syndrome. *Am. J. Med. Genet. A* **155A**, 2479–2483 (2011).
19 Chiesa, N., De Crescenzo, A., Mishra, K., Perone, L., Carella, M. & Palumbo, O. *et al.* The KCNQ1OT1 imprinting control region and non-coding RNA: new properties derived from the study of Beckwith-Wiedemann syndrome and Silver–Russell syndrome cases. *Hum. Mol. Genet.* **21**, 10–25 (2012).

Supplementary Information accompanies the paper on Journal of Human Genetics website (http://www.nature.com/jhg)

European Journal of Human Genetics (2008) 0, 000–000

www.nature.com/ejhg

SHORT REPORT

Epimutation (hypomethylation) affecting the chromosome 14q32.2 imprinted region in a girl with upd(14)mat-like phenotype

Kana Hosoki[1], Tsutomu Ogata*[,2], Masayo Kagami[2], Touju Tanaka[3] and Shinji Saitoh[1]

[1]*Department of Pediatrics, Hokkaido University Graduate School of Medicine, Sapporo, Japan;* [2]*Department of Endocrinology and Metabolism, National Research Institute for Child Health and Development, Tokyo, Japan;* [3]*Division of Clinical Genetics and Molecular Medicine, National Center for Child Health and Development, Tokyo, Japan*

Maternal uniparental disomy for chromosome 14 (upd(14)mat) causes clinically discernible features such as pre- and/or postnatal growth failure, hypotonia, obesity, small hands, and early onset of puberty. The monoallelic expression patterns at the 14q32.2 imprinted region are tightly related to methylation status of the *DLK1–MEG3* intergenic differential methylation region (DMR) and the *MEG3*-DMR that are severely hypermethylated after paternal transmission and grossly hypomethylated after maternal transmission. We examined this imprinted region in a 2 2/12-year-old Japanese patient who was born with a normal birth size (length, +0.2 SD; weight, −0.5 SD) and showed postnatal growth failure (height, −3.1 SD; weight, −3.4 SD), hypotonia, frontal bossing, micrognathia, and small hands. Methylation analysis, genotyping analysis, and deletion analysis were performed with blood samples of the patient and the parents, showing that the DMRs of this patient were grossly hypomethylated in the absence of upd(14)mat and deletion of the DMRs. The results indicate the occurrence of an epimutation (hypomethylation) affecting the normally methylated DMRs of paternal origin, and imply that epimutations should be examined in patients with upd(14)mat-like phenotype.
European Journal of Human Genetics (2008) **0**, 000–000. doi:10.1038/ejhg.2008.90

Keywords: epimutation; growth failure; imprinting; differentially methylated region; upd(14)mat

Introduction

Maternal uniparental disomy for chromosome 14 (upd(14)mat) results in clinically discernible features such as pre- and postnatal growth failure, hypotonia, obesity, small hands, and early onset of puberty.[1] Phenotypic development is consistent with chromosome 14q32.2 region harboring several paternally expressed genes (*PEGs*) such as *DLK1* and *RTL1* and maternally expressed genes (*MEGs*) such as *MEG3* (alias *GTL2*), *RTL1as* (*RTL1* antisense), and *MEG8*.[2,3] The parent-of-origin-specific monoallelic expression patterns are tightly related to methylation status of differential methylation regions (DMRs).[4] For the 14q32.2 imprinted region, the previous studies have identified the intergenic DMR (IG-DMR) between *DLK1* and *MEG3* and the *MEG3*-DMR that are severely hypermethylated after paternal transmission and grossly hypomethylated after maternal transmission.[5–7] In particular, the germline-derived IG-DMR plays a pivotal role in the imprinting regulation, because methylation pattern of the secondary *MEG3*-DMR is dependent on that of the IG-DMR.[8]

The upd(14)mat-like phenotype has also been exhibited by non-disomic patients. Temple *et al*[9] described a patient

*Correspondence: Dr T ogata, Department of Endocrinology and Metabolism, National Research Institute for Child Health and Development, 2-10-1 Ohkura, Setagaya, Tokyo 157-8535, Japan.
Tel: +81 2 5494 7025; Fax: +81 2 5494 7026;
E-mail: tomogata@nch.go.jp
Received 10 January 2008; revised 25 March 2008; accepted 3 April 2008

with upd(14)mat-like phenotype and an epimutation (hypomethylation) of the normally methylated DMR of paternal origin. Kagami *et al*[5] reported three patients with upd(14)mat-like phenotype and microdeletions affecting the 14q32.2 imprinted region including the DMRs of paternal origin. In this regard, the IG-DMR deletion from the paternally derived chromosome has no effect on the imprinting status, although that from the maternally derived chromosome results in a maternal to paternal epigenotypic alteration.[5,7] Thus, simple genotype–phenotype correlations can be applied for the three patients with the microdeletions, implying that loss of paternally derived *DLK1* and *RTL1* constitutes primary additive underlying factors for the development of upd(14)mat-like phenotype, although the perturbation of other imprinted genes could also have some effects.[5]

Here, we report an epimutation identified in a patient with upd(14)mat-like phenotype.

Patient and methods

Case report

This Japanese girl was born at 41 weeks of gestation after natural conception, with a history of mild oligohydramnios in the third trimester. At birth, her length was 50.0 cm (+0.2 SD), her weight 3.03 kg (−0.5 SD), and her head circumference 34.5 cm (+0.8 SD). The non-consanguineous parents were clinically normal, and the height was 161.0 cm (−1.7 SD) for the father and 154.5 cm (−0.7 SD) for the mother.

At 5 months of age, she was referred to us, because she was unable to control her head. Physical examination revealed generalized hypotonia without palsy and abnormal tendon reflex, and several somatic features such as frontal bossing, micrognathia, and small hands (Supplementary Figure 1). In addition, her length became below −2 SD of the mean from 10 months of age, while hypotonia was gradually ameliorated. She controlled her head at 7 months of age, sat without support at 11 month, and walked without support at 19 months. Repeatedly performed biochemical studies for hypotonia and growth failure were normal, as were skeletal roentgenograms and brain magnetic resonance imaging. The karyotype was 46XX in all the 30 lymphocytes examined. With a provisional diagnosis of Prader–Willi syndrome (PWS) that is primarily based on hypotonia and growth deficiency, fluorescence *in situ* hybridization (FISH) analysis for *SNRPN* and methylation analysis for the DMR at the *SNRPN* promoter region were performed,[10] showing normal findings. In addition, hypomethylation of the *H19*-DMR and upd(7)mat, which can cause growth failure, were also excluded by previous methods.[11,12] On the last examination at 2 2/12 years of age, her height was 76.1 cm (−3.1 SD), her weight 7.9 kg (−3.4 SD), and her head circumference 44.9 cm (−1.9 SD). Her mental development appeared age appropriate.

Methylation analysis

This study was approved by the Institutional Review Board Committees at Hokkaido University Hospital and National Center for Child Health and Development. After obtaining written informed consent, we examined the IG-DMR (CG4 and CG6) and the *MEG3*-DMR (Figure 1a), using bisulfite-treated leukocyte genomic DNA. For the IG-DMR, bisulfite sequencing was performed as reported previously,[5] and the SNPs (*rs12437020* for CG4 and *rs10133627* for CG6) were also genotyped. For the *MEG3*-DMR, PCR amplification was performed with methylated and unmethylated allele-specific primers, as described previously.[5,6] A hitherto unreported upd(14)mat patient and the previously reported upd(14)pat patient[5] were similarly analyzed with permission.

Genotyping analysis

We performed microsatellite analysis for 16 loci on chromosome 14 and SNP analysis for 39 loci around the DMRs (Supplementary Table 1). The primers used were as reported previously.[5]

Deletion analysis

Lymphocyte metaphase spreads were hybridized with a long and accurate (LA)-PCR product encompassing the IG-DMR (FISH probe 1) and that spanning the *MEG3*-DMR (Figure 1a), together with an RP11-566I2 probe for 14q12 used as an internal control. Furthermore, the two LA-PCR products were also obtained from the patient and a control subject, and subjected to fragment size comparisons after restriction enzyme digestions, to detect a possible tiny deletion in the patient. The detailed methods for the deletion analysis have been reported previously.[5]

Results

Methylation analysis

The results are shown in Figure 1b. For the IG-DMR, CG4 and CG6 were grossly hypomethylated in the patient and the upd(14)mat patient, severely methylated in the upd(14)pat patient, and delineated in apparently mosaic patterns in the parents. In addition, the CG4 SNP typing indicated parental origin-dependent methylation patterns in the parents, and heterodisomy for the this region in the upd(14)mat patient. The CG6 SNP typing data were not informative. For the *MEG3*-DMR, PCR products were obtained with an unmethylated allele-specific primer pair alone in the patient and the upd(14)mat patient, with a methylated allele-specific primer pair alone in the upd(14)pat patient, and with both primer pairs in the parents.

NPG.EJHG.EJHG200890

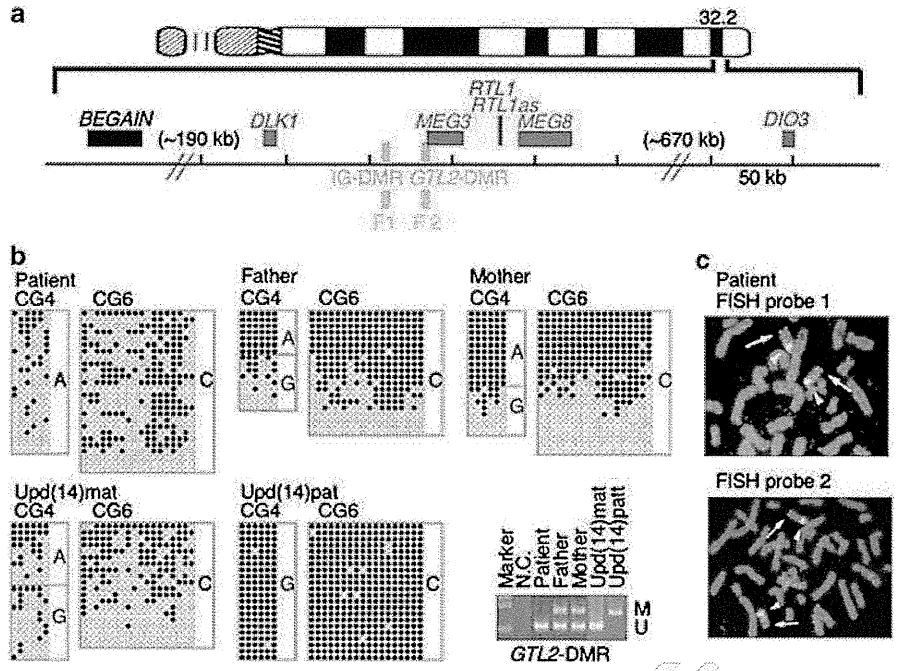

Figure 1 Summary of the molecular studies. (**a**) The regional physical map of the human chromosome 14q32.2 imprinted region. *PEGs* are shown in blue and *MEGs* in red; although it remains to be clarified whether *DIO3* is a *PEG*, mouse *Dio3* is known to be preferentially but not exclusively expressed from a paternally derived chromosome in embryos.[13] *WDR25* and *BEGAIN* appear biparentally expressed genes. The IG-DMR and the *MEG3*-DMR are depicted in green, and the FISH probes 1 and 2 covering the DMRs indicated in orange. The physical distance is ~190 kb between *BEGAIN* and *DLK1*, ~170 kb between *DLK1* and *MEG8*, and ~670 kb between *MEG8* and *DIO3*. (**b**) Methylation patterns of the IG-DMR (CG4 and CG6) and the *MEG3*-DMR. Bisulfite sequencing has been performed for CG4 and CG6. Each line indicates a single clone and each circle denotes a CpG island; filled and open circles represent methylated and unmethylated cytosines, respectively. The SNP typing data for CG4 and CG6 are also shown. Methylated (M) and unmethylated (U) allele-specific PCR amplification has been performed for the *MEG3*-DMR. NC: negative control. (**c**) FISH analysis using FISH probe 1 (F1) for the IG-DMR and FISH probe 2 (F2) for the *MEG3*-DMR. The red signals (arrows) have been detected by the two FISH probes and the green signals (arrowheads) have been identified by an RP11-566I2 probe for 14q12 used as an internal control.

Genotyping analysis

Microsatellite analysis demonstrated biparental origin of the two chromosome 14 homologs, and SNP analysis indicated lack of a segmental upd(14)mat around the DMRs (Supplementary Table 1).

Deletion analysis

FISH probes 1 and 2 detected two signals in the patient (Figure 1c). The fragment size comparison after enzyme digestions showed no abnormal bands suggestive of a tiny deletion in the patient.

Discussion

This patient had hypomethylated DMRs in the absence of discernible maternal disomy affecting the DMRs or loss of the paternally derived DMRs. This implies the occurrence of an epimutation (hypomethylation) affecting the normally methylated DMRs of paternal origin. To our knowledge, such an epimutation (hypomethylation) has previously been identified only in a patient reported by Temple *et al.*[9] Actually, the DMR examined in that patient appears to be a part of the *MEG3*-DMR rather than the IG-DMR on the basis of its position. It is likely, however, that the IG-DMR is also hypomethylated in that patient, because the *MEG3*-DMR can stay hypomethylated only in the presence of the hypomethylated IG-DMR.[8]

Clinical features of the two patients with epimutation are summarized in Table 1, together with those of upd(14)mat patients. Notably, clinical features are grossly similar in epimutation patients and upd(14)mat patients. Although our patient had no prenatal growth failure, lack of prenatal and/or postnatal growth failure has been described in several upd(14)mat patients,[14–16] and this would be due to body growth being a multifactorial trait subject to multiple genetic and environmental factors.[17] In this regard, it has been reported that clinical features are comparable between patients with paternal upd(14) and those with epimutations (hypermethylation) affecting the normally hypomethylated DMRs of maternal origin.[5] Taken together, the methylation patterns of the DMRs appear to be closely related to the expression patterns of virtually all the imprinted genes on 14q32.2.

It is noteworthy that the patient was initially suspected as having PWS. Indeed, growth deficiency, hypotonia, and small hands are shared by upd(14)mat and PWS,[18,19] and

NPG.EJHG.EJHG200890

Table 1 Clinical phenotypes in patients with epimutations and upd(14)mat

	Epimutations		*Upd(14)mat*
	This report	*Temple* et al[9]	(n = 35)[a]
Age	2 2–12 years	10 7–12 years	0–30 years
Sex	Female	Male	M:F = 17:18
Premature delivery	–	–	10/25
Prenatal growth failure	–	+	24/27
Postnatal growth failure	+	+	26/32
Somatic features	+	+	23/35[b]
Frontal bossing	+	+	9/9
High arched palate	–	+	7/9
Micrognathia	+	–	5/5
Small hands	+	+	24/27
Scoliosis	–	+	5/19
Others			
Hypotonia	+	+	25/28
Obesity	–	–	14/34
Early onset of puberty	Unknown	Borderline	14/16
Mental retardation	–	–	10/27
Thyroid dysfunction	–	–	ND

ND: not described.
In the column summarizing the clinical features of 35 patients with upd(14)mat, the denominators indicate the number of patients examined for the presence or absence of each feature, and the numerators represent the number of patients assessed to be positive for that feature; thus, the differences between the denominators and the numerators denote the number of patients evaluated to be negative for that feature.
[a]Patients with maternal uniparental disomy for chromosome 14 reported in the literature, several upd(14)mat patients with no phenotypic description have not been included. The references for the 35 upd(14)mat patients are summarized in Kagami *et al*.[5]
[b]The ratio of patients with at least one somatic feature.

upd(14)mat has occasionally been identified in patients referred for molecular examination of PWS.[19,20] Thus, upd(14)mat and epimutations should be considered in patients with PWS-like phenotype.[18,19]

In summary, we observed an epimutation (hypomethylation) of the paternally derived DMRs in a patient with upd(14)mat-like phenotype. Further studies will identify epimutations in patients with upd(14)mat-like phenotype, thereby contributing to clarify the relevance of epimutations in human imprinted disorders.

Acknowledgements

This study was supported by grants for Child Health and Development (20C-2) and for Research on Children and Families (H18-005) from the Ministry of Health, Labor, and Welfare, and by Grants-in-Aid for Scientific Research (Priority Areas: 16086215) from the Ministry of Education, Culture, Sports, Science and Technology.

Disclosure

The authors have reported no conflicts of interest.

References

1 Kotzot D: Maternal uniparental disomy 14 dissection of the phenotype with respect to rare autosomal recessively inherited traits, trisomy mosaicism, and genomic imprinting. *Ann Genet* 2004; **47**: 251–260.
2 Cavaille J, Seitz H, Paulsen M, Ferguson-Smith AC, Bachellerie JP: Identification of tandemly-repeated C/D snoRNA genes at the imprinted human 14q32 domain reminiscent of those at the Prader-Willi/Angelman syndrome region. *Hum Mol Genet* 2002; **11**: 1527–1538.
3 Charlier C, Segers K, Wagenaar D *et al*: Human-ovine comparative sequencing of a 250-kb imprinted domain encompassing the callipyge (clpg) locus and identification of six imprinted transcripts: DLK1, DAT, GTL2, PEG11, antiPEG11, and MEG8. *Genome Res* 2001; **11**: 850–862.
4 Li E, Beard C, Jaenisch R: Role for DNA methylation in genomic imprinting. *Nature* 1993; **366**: 362–365.
5 Kagami M, Sekita Y, Nishimura G *et al*: Deletions and epimutations affecting the human chromosome 14q32.2 imprinted region: implications for the phenotypic development in paternal and maternal uniparental disomy for chromosome 14. *Nat Genet* e-pub ahead of print.
6 Murphy SK, Wylie AA, Coveler KJ *et al*: Epigenetic detection of human chromosome 14 uniparental disomy. *Hum Mutat* 2003; **22**: 92–97.
7 Lin SP, Youngson N, Takada S *et al*: Asymmetric regulation of imprinting on the maternal and paternal chromosomes at the Dlk1-Gtl2 imprinted cluster on mouse chromosome 12. *Nat Genet* 2003; **35**: 97–102.
8 Takada S, Paulsen M, Tevendale M *et al*: Epigenetic analysis of the Dlk1-Gtl2 imprinted domain on mouse chromosome 12: implications for imprinting control from comparison with Igf2-H19. *Hum Mol Genet* 2002; **11**: 77–86.
9 Temple IK, Shrubb V, Lever M, Bullman H, Mackay DJ: Isolated imprinting mutation of the DLK1/GTL2 locus associated with a clinical presentation of maternal uniparental disomy of chromosome 14. *J Med Genet* 2007; **44**: 637–640.
10 The ASHG/ACMG Test and Technology Transfer Committee: Diagnostic testing for Prader–Willi and Angelman syndromes. *Am J Hum Genet* 1996; **58**: 1085–1088.

NPG.EJHG.EJHG200890

11 Kagami M, Nagai T, Fukami M, Yamazawa K, Ogata T: Silver-Russell syndrome in a girl born after *in vitro* fertilization: partial hypermethylation at the differentially methylated region of PEG1/MEST. *J Assist Reprod Genet* 2007; **24**: 131–136.
12 Yamazawa K, Kagami M, Ogawa M, Horikawa R, Ogata T: Placental hypoplasia in maternal uniparental disomy for chromosome 7. *Am J Med Genet A* 2008; **146**: 514–516.
13 Tsai CE, Lin SP, Ito M, Takagi N, Takada S, Ferguson-Smith AC: Genomic imprinting contributes to thyroid hormone metabolism in the mouse embryo. *Curr Biol* 2002; **12**: 1221–1226.
14 Rosa AL, Wu YQ, Kwabi-Addo B, Coveler KJ, Reid Sutton V, Shaffer LG: Allele-specific methylation of a functional CTCF binding site upstream of MEG3 in the human imprinted domain of 14q32. *Chromosome Res* 2005; **13**: 809–818.
15 Aretz S, Raff R, Woelfle J *et al*: Maternal uniparental disomy 14 in a 15-year-old boy with normal karyotype and no evidence of precocious puberty. *Am J Med Genet A* 2005; **135**: 336–338.
16 Takahashi I, Takahashi T, Utsunomiya M, Takada G, Koizumi A: Long-acting gonadotropin-releasing hormone analogue treatment for central precocious puberty in maternal uniparental disomy chromosome 14. *Tohoku J Exp Med* 2005; **207**: 333–338.
17 Vogel F, Motulsky AG: *Human Genetics: Problems and Approaches*. Heidelberg: Springer-Verlag, 1986.
18 Gunay-Aygun M, Schwartz S, Heeger S, O'Riordan MA, Cassidy SB: The changing purpose of Prader–Willi syndrome clinical diagnostic criteria and proposed revised criteria. *Pediatrics* 2001; **108**: E92.
19 Berends MJ, Hordijk R, Scheffer H, Oosterwijk JC, Halley DJ, Sorgedrager N: Two cases of maternal uniparental disomy 14 with a phenotype overlapping with the Prader–Willi phenotype. *Am J Med Genet* 1999; **84**: 76–79.
20 Mitter D, Buiting K, von Eggeling F *et al*: Is there a higher incidence of maternal uniparental disomy 14 [upd(14)mat]? Detection of 10 new patients by methylation-specific PCR. *Am J Med Genet A* 2006; **140**: 2039–2049.

Supplementary Information accompanies the paper on European Journal of Human Genetics website (http://www.nature.com/ejhg)

NPG.EJHG.EJHG200890

5. Longston L, Laws JW. Dysphagia in carcinoma of the pancreas. *J Faculty Radiol.* 1954;6: 134–138.
6. Fisher M. Metastasis to the esophagus. *Gastrointest Radiol.* 1976;1: 249–251.
7. Mizobuchi S, Tachimori Y, Kato H, et al. Metastatic esophageal tumors from distant primary lesions: report of three esophagectomies and study of 1835 autopsy cases. *Jpn J Clin Oncology.* 1997;27: 410–414.
8. Sanborn EB, Beattie EJ Jr, Slaughter DP. Secondary neoplasms of the mediastinum. *J Thorac Surg.* 1958;35:678–682.
9. Simchuk EJ, Low DE. Direct esophageal metastasis from a distant primary tumor is a submucosal process: a review of six cases. *Dis Esophagus.* 2001;14: 247–250.
10. Sunada F, Yamamoto H, Kita H, et al. A case of esophageal stricture due to metastatic breast cancer diagnosed by endoscopic mucosal resection. *Jpn J Clin Oncol.* 2005;35:483–486.

Variants in the Interferon Regulatory Factor-2 Gene Are Not Associated With Pancreatitis in Japan

To the Editor:

Since the identification of mutations in the cationic trypsinogen (protease, serine, 1; *PRSS1*) gene as a cause of hereditary pancreatitis in 1996,[1] several pancreatitis susceptibility genes have been identified.[2–4] Gain-of-function mutations in the cationic trypsinogen (protease, serine, 1; *PRSS1*) gene as well as loss-of-function variants in the serine protease inhibitor Kazal type 1 gene and the trypsin-degrading enzyme chymotrypsin C increase the risk for chronic pancreatitis (CP).[1–3] In 2013, carboxypeptidase A1 was identified as a novel pancreatitis susceptibility gene.[4] However, in our nationwide survey of hereditary pancreatitis in Japan,[5] about 30% of the families have no mutations in either of these pancreatitis susceptibility genes, indicating that other, still unknown, susceptibility genes exist.

Interferon regulatory factor-2 (IRF2) is a member of a family of transcriptional factors involved in the modulation of interferon-induced immune responses to viral infection.[6] Recent studies using mice deficient for *Irf2* have uncovered a role of IRF2 in pancreatitis.[7,8] In the pancreatic acinar cells of $Irf2^{-/-}$ mice, (1) zymogen granules were densely localized throughout the cytoplasm, (2) regulated exocytosis was abolished, (3) the expression of soluble *N*-ethylmaleimide-sensitive factor attachment protein receptor proteins was altered, and (4) autophagy was activated.[7] Poly(I:C), a synthetic double-stranded RNA, induced severe pancreatitis in $Irf2^{-/-}$, but not in wild-type mice.[8] Trypsinogen5 messenger RNA (mRNA) was constitutively up-regulated about 1000-fold in $Irf2^{-/-}$ mice compared with controls. These findings prompted us to examine whether variants in the *IRF2* gene are associated with pancreatitis.

Exons and the flanking regions for the coding regions in the *IRF2* gene were amplified by polymerase chain reaction and directly sequenced in 172 patients with alcoholic CP, 200 patients with nonalcoholic CP (153 idiopathic, 29 hereditary, 13 familial, 5 divisum), and 276 controls. All subjects were Japanese. This study was approved by the Ethics Committee of Tohoku University School of Medicine (article#2012-1-158).

In our cohort of 372 CP patients, we identified 4 variants in the coding region of the *IRF2* gene (Table 1). Three variants (c.123G>A, c.651C>T, c.744G>A) were synonymous, and one variant (c.638C>T, p.P213L) was nonsynonymous. The c.123G>A variant was not described before, neither in the published literature nor in the Human Genome Mutation Database. There was no significant difference for any of the variants detected between the CP patients and control group.

Genetic variants, including the c.744G>A, in the *IRF2* gene have been shown to be associated with psoriasis, atopic dermatitis, and eczema herpeticum.[9,10] Because the c.744G>A variant is located at the +3 position of exon 9, this variant might affect the splicing machinery.[10] The *A* allele of this variant was predicted to bind to the serine/arginine-rich family member ASF/SF2, a pre-mRNA splicing factor playing a role in mRNA stability.[9] Nevertheless, exonic variants, including the c.744G>A, in the *IRF2* gene were not associated with pancreatitis, suggesting that *IRF2* is not likely to be a pancreatitis susceptibility gene in humans.

ACKNOWLEDGMENT

Supported in part by the Pancreas Research Foundation of Japan (to Dr Nakano), the HIROMI Medical Research Foundation (to Dr Masamune), the Mother and Child Health Foundation (to Dr Masamune), and the Research Committee of Intractable Pancreatic Diseases provided by the Ministry of Health, Labour, and Welfare of Japan.

TABLE 1. Frequency of the Exonic IRF2 Variants in Japanese Patients With CP and Controls

IRF2 Exonic Variants	Genotype	Total CP, %	Alcoholic CP, %	Nonalcoholic CP, %	Controls, %	*P* (Total CP vs Controls)*
Exon 3						
c.123G>A (p.A41=)	GA	1/372 (0.3)	0/172 (0)	1/200 (0.5)	0/276 (0)	>0.99
Exon 7						
c.638C>T (p.P213L)	CT	2/372 (0.5)	0/172 (0)	2/200 (1.0)	1/276 (0.4)	>0.99
c.651C>T (p.S217=)	CT	2/372 (0.5)	0/172 (0)	2/200 (1/0)	2/276 (0.7)	>0.99
Exon 9						
c.744G>A (p.G248=)	GA	179/372 (48.1)	85/172 (49.4)	94/200 (47.0)	142/276 (51.4)	0.64
	AA	45/372 (12.1)	19/172 (11.0)	26/200 (13.0)	34/276 (12.3)	

*Fisher exact test.

The authors declare no conflict of interest.

Eriko Nakano, MD
Atsushi Masamune, MD, PhD
Kiyoshi Kume, MD, PhD
Yoichi Kakuta, MD, PhD
Tooru Shimosegawa, MD, PhD
Division of Gastroenterology
Tohoku University Graduate
School of Medicine
Sendai, Japan
amasamune@med.tohoku.ac.jp

REFERENCES

1. Whitcomb DC, Gorry MC, Preston RA, et al. Hereditary pancreatitis is caused by a mutation in the cationic trypsinogen gene. *Nat Genet.* 1996;14:141–145.
2. Witt H, Luck W, Hennies HC, et al. Mutations in the gene encoding the serine protease inhibitor, Kazal type 1 are associated with chronic pancreatitis. *Nat Genet.* 2000;25: 213–216.
3. Rosendahl J, Witt H, Szmola R, et al. Chymotrypsin C (CTRC) variants that diminish activity or secretion are associated with chronic pancreatitis. *Nat Genet.* 2008;40: 78–82.
4. Witt H, Beer S, Rosendahl J, et al. Variants in CPA1 are strongly associated with early onset chronic pancreatitis. *Nat Genet.* 2013;45: 1216–1220.
5. Masamune A. Genetics of pancreatitis: the 2014 update. *Tohoku J Exp Med.* 2014;232: 69–77.
6. Savitsky D, Tamura T, Yanai H, et al. Regulation of immunity and oncogenesis by the IRF transcription factor family. *Cancer Immunol Immunother.* 2010;59:489–510.
7. Mashima H, Sato T, Horie Y, et al. Interferon regulatory factor-2 regulates exocytosis mechanisms mediated by SNAREs in pancreatic acinar cells. *Gastroenterology.* 2011;141: 1102–1113.
8. Hayashi H, Kohno T, Yasui K, et al. Characterization of dsRNA-induced pancreatitis model reveals the regulatory role of IFN regulatory factor 2 (Irf2) in trypsinogen5 gene transcription. *Proc Natl Acad Sci U S A.* 2011;108: 18766–18771.
9. Gao PS, Leung DY, Rafaels NM, et al. Genetic variants in interferon regulatory factor 2 (IRF2) are associated with atopic dermatitis and eczema herpeticum. *J Invest Dermatol.* 2012;132:650–657.
10. Foerster J, Nolte I, Schweiger S, et al. Evaluation of the *IRF-2* gene as a candidate for PSORS3. *J Invest Dermatol.* 2004;122:61–64.

Establishment of an Orthotopic Model of Pancreatic Cancer to Evaluate the Antitumor Effects of Irinotecan Through the Biomarker Carbohydrate Antigen 19-9 in Mice

To the Editor:

The level of carbohydrate antigen 19-9 (CA19-9, also called *cancer antigen 19-9*) is elevated in many types of gastrointestinal cancers, such as hepatocellular carcinoma, as well as colorectal, esophageal, and pancreatic cancers.[1] As a tumor marker in symptomatic patients with pancreatic cancer, CA19-9 has a sensitivity of 70% to 80% and a specificity of 80% to 90%.[2] However, its use as a cancer screening tool, particularly for pancreatic cancer screening, is discouraged by the American Society of Clinical Oncology because of the risk for false-negatives or false-positives. Therefore, the main use of CA19-9 is to monitor responses to therapies.[1,3,4]

In current preclinical studies, tumor size (weight) from xenograft models remains the only indicator for drug efficacy evaluation. To our knowledge, there has not yet been an effective demonstration of a plasma biomarker for therapy response in tumor-bearing animals. In view of this, development of an orthotopic xenograft model of pancreatic cancer to evaluate the efficiency of chemotherapeutic agents through the biomarker CA19-9 becomes very attractive.

MATERIALS AND METHODS

Carbohydrate antigen 19-9 expression and secretion in cell culture media in 4 human pancreatic adenocarcinoma cell lines, PANC-1, CAPAN-1, CAPAN-2, and SW1990, were detected by Western blotting and enzyme-linked immunosorbent assay (ELISA), respectively. SW1990 cells were implanted into the pancreata of BALB/c nude mice. On the eighth day after orthotopic implantation, the animals were randomly divided into vehicle control group (13 mice) or treatment group (11 mice). The treatment group was injected with 25 mg/kg of irinotecan (CPT-11) twice a week. To exclude the effects of the surgical operation, a sham group received the same operation procedures but with only phosphate buffered saline injected into the pancreata. After 3 weeks of treatment, the mice were sacrificed and the tumors were excised and weighed. The concentration of CA19-9 in plasma of the mice was measured by ELISA kit. Differences were considered to be statistically significant when $P < 0.05$. The cryosections of pancreata (tumors) in each group (sham, control, or CPT-11 treatment group) were used for assessing CA19-9 expression by immunostaining.

RESULTS

SW1990 Cells Overexpressed and Secreted CA19-9

Western blotting showed that SW1990 cells overexpressed CA19-9, whereas the other 3 pancreatic cancer cell lines did not (Fig. 1A). In addition, the media from SW1990 cells also contained significantly higher levels of CA19-9 by ELISA detection (Fig. 1B). Therefore, SW1990 cells were used for our orthotopic xenograft pancreatic cancer model.

Irinotecan Inhibited the Growth of SW1990 Human Pancreatic Tumor Xenografts and Decreased the Levels of the Biomarker CA19-9 in Plasma and Tumor Tissues

The weights of the pancreata from the control group animals were significantly higher than those of the sham group, which was not implanted with cancer cells ($P < 0.001$; Figs. 1C, E), demonstrating that orthotopic pancreatic tumors were successfully developed in the pancreata of nude mice. After the treatment with CPT-11 (25 mg/kg, twice per week) for 3 weeks, the weights of pancreata (including tumor) of the mice were significantly lower than those of the control group ($P < 0.001$; Figs. 1C, E).

The levels of the biomarker CA19-9 in plasma, which should be elevated if the pancreatic tumor existed,[3] were assessed. The concentration of CA19-9 in the sham group was lower than the detection limit of the kit, which was 10 U/mL. The mean (SD) concentration of CA19-9 in the control group was 116 (33.7) U/mL (n = 13), which was significantly higher than that of the sham group (Fig. 1D). These results demonstrated that the induction of pancreatic tumor growth by inoculation of SW1990 cells could be reflected by a rise in CA19-9 level. Furthermore, treatment with CPT-11 significantly decreased the CA19-9 levels in plasma ($P < 0.05$) (Fig. 1D). Therefore, the levels of CA19-9

Dig Dis Sci
DOI 10.1007/s10620-014-3476-9

ORIGINAL ARTICLE

Targeted Next-Generation Sequencing Effectively Analyzed the Cystic Fibrosis Transmembrane Conductance Regulator Gene in Pancreatitis

Eriko Nakano · Atsushi Masamune · Tetsuya Niihori · Kiyoshi Kume · Shin Hamada · Yoko Aoki · Yoichi Matsubara · Tooru Shimosegawa

Received: 5 September 2014 / Accepted: 28 November 2014

Abstract
Background The cystic fibrosis transmembrane conductance regulator (*CFTR*) gene, responsible for the development of cystic fibrosis, is known as a pancreatitis susceptibility gene. Direct DNA sequencing of PCR-amplified *CFTR* gene segments is a first-line method to detect unknown mutations, but it is a tedious and labor-intensive endeavor given the large size of the gene (27 exons, 1,480 amino acids). Next-generation sequencing (NGS) is becoming standardized, reducing the cost of DNA sequencing, and enabling the generation of millions of reads per run. We here report a comprehensive analysis of *CFTR* variants in Japanese patients with chronic pancreatitis using NGS coupling with target capture.
Methods Exon sequences of the *CFTR* gene from 193 patients with chronic pancreatitis (121 idiopathic, 46 alcoholic, 17 hereditary, and nine familial) were captured by HaloPlex target enrichment technology, followed by NGS.
Results The sequencing data covered 91.6 % of the coding regions of the *CFTR* gene by ≥20 reads with a mean read depth of 449. We could identify 12 non-synonymous variants including three novel ones [c.A1231G (p.K411E), c.1753G>T (p.E585X) and c.2869delC (p.L957fs)] and seven synonymous variants including three novel ones in the exonic regions. The frequencies of the c.4056G>C (p.Q1352H) and the c.3468G>T (p.L1156F) variants were higher in patients with chronic pancreatitis than those in controls.
Conclusions Target sequence capture combined with NGS is an effective method for the analysis of pancreatitis susceptibility genes.

Keywords Chloride channel · HaloPlex · In silico analysis · MiSeq · Target enrichment

Abbreviations

bp	Base pair
CF	Cystic fibrosis
CFTR	Cystic fibrosis transmembrane conductance regulator
CP	Chronic pancreatitis
ERCP	Endoscopic retrograde cholangiopancreatography
NGS	Next-generation sequencing
PCR	Polymerase chain reaction
RD	Related disorder
SIFT	Sorting Intolerant From Tolerant

Introduction

Chronic pancreatitis (CP) is a progressive inflammatory disease that eventually leads to impairment of the exocrine and endocrine functions of the organ [1, 2]. Since the identification of mutations in the cationic trypsinogen

E. Nakano · A. Masamune (✉) · K. Kume · S. Hamada · T. Shimosegawa
Division of Gastroenterology, Tohoku University Graduate School of Medicine, 1-1 Seiryo-machi, Aoba-ku, Sendai 980-8574, Japan
e-mail: amasamune@med.tohoku.ac.jp

T. Niihori · Y. Aoki · Y. Matsubara
Department of Medical Genetics, Tohoku University Graduate School of Medicine, Sendai 980-8574, Japan

Y. Matsubara
National Research Institute for Child Health and Development, Tokyo 157-8535, Japan

Published online: 10 December 2014

(protease, serine, 1; *PRSS1*) gene as a cause of hereditary pancreatitis in 1996 [3], several pancreatitis susceptibility genes have been identified [3–6]. Gain-of-function mutations in the *PRSS1* gene as well as loss-of-function variants in the serine protease inhibitor Kazal type 1 (*SPINK1*) gene and the trypsin-degrading enzyme chymotrypsin C (*CTRC*) increase the risk of CP [3–5]. In 2013, carboxypeptidase A1 (*CPA1*) gene was identified as a novel pancreatitis susceptibility gene [6]. These studies have been replicated in the Japanese population [7–10].

The cystic fibrosis transmembrane conductance regulator (*CFTR*) gene is another pancreatitis susceptibility gene [11, 12]. Acute recurrent pancreatitis and CP have been accepted as CFTR-related disorders (CFTR-RDs), a clinical entity associated with CFTR dysfunction that does not fulfill the diagnostic criteria for cystic fibrosis (CF; MIM# 219700) [13]. The *CFTR* gene, responsible for the development of CF, encodes for a cyclic adenosine monophosphate-dependent chloride channel that is located in the apical membrane of secretory and absorptive epithelial cells of the pancreas, intestine, liver, airways, vas deferens, and sweat glands [14]. In general, the clinical manifestations of CF arise from ductal and glandular obstruction because of an inability to hydrate macromolecules within the ductal lumens [15]. Until now, more than 1,900 variants have been identified in the Cystic Fibrosis Mutation Database (http://www.genet.sickkids.on.ca/cftr). The human *CFTR* gene spans 250 kb and contains 27 exons that encode for a protein with a total length of 1,480 amino acids [14]. Direct DNA sequencing of polymerase chain reaction (PCR)-amplified *CFTR* gene segments is a first-line method to detect unknown *CFTR* mutations [16], but this is a tedious and labor-intensive endeavor given the large size of the gene.

A new approach that uses massive parallel sequencing called next-generation sequencing (NGS) is becoming standardized, and the cost is rapidly dropping [17]. Using the ultimate platforms, such systems are able to perform billions of sequencing reactions with a read length of 150–250 nucleotides. For most research groups, whole-genome sequencing of many samples remains a costly endeavor, and targeted capture of selected regions of interest followed by sequencing provides a more efficient and cost-effective option. This strategy has allowed identification of causal variants in several Mendelian disorders, variants associated with complex diseases, and recurrently mutated cancer genes [18–20]. The HaloPlex target enrichment technology is a selective circularization-based method that is a further development of the principle of selector probes [21]. In the HaloPlex technology, genomic DNA is fragmented by restriction enzyme digestion and circularized by hybridization to probes whose ends are complementary to the target fragments. Compared to hybrid capture methods, the HaloPlex system requires smaller amounts of starting DNA, has higher specificity (fraction of sequence reads in the region of interest), and provides more uniform genome coverage [22]. Using the bench-top Illumina MiSeq platform, comprehensive analysis of many samples can be easily done. We here report the comprehensive analysis of *CFTR* variants in Japanese patients with CP.

Materials and Methods

Subjects

One hundred and ninety-three patients with CP (121 idiopathic, 46 alcoholic, 17 hereditary, and nine familial) were enrolled in this study. Because we initially aimed to identify novel pancreatitis-associated genes using the HaloPlex system, majority of the patients recruited were nonalcoholic. To extend our findings, we additionally recruited patients with alcoholic CP who had developed CP at relatively younger ages (mean: 44.1 years old). The diagnosis of CP was based on at least two separate episodes of abdominal pain and radiological findings of pancreatic calcifications by computed tomography, endoscopic ultrasonography, and/or morphological findings such as pancreatic ductal irregularities and dilatations revealed by endoscopic retrograde cholangiopancreatography (ERCP) or by magnetic resonance imaging [23]. Hereditary pancreatitis was diagnosed when one first-degree relative or two or more second-degree relatives had recurrent acute pancreatitis or CP without any apparent predisposing factor [24]. Patients with CP in whom the criteria for hereditary pancreatitis were not met but who had at least two affected family members were classified as having familial pancreatitis. Idiopathic CP was diagnosed in the absence of a positive family history or possible predisposing factors such as alcohol abuse, trauma, medication, and anatomical abnormalities. Patients who consumed alcohol over 80 g/day (for men) or 60 g/day (for women) for more than 2 years were classified as alcoholic CP. All subjects were Japanese. This study was performed with the informed consent of the patients in accordance with the principles of the declaration of Helsinki. This study was approved by the Ethics Committee of Tohoku University School of Medicine (article#: 2013-1-498).

Peripheral Blood Collection and DNA Preparation

After written informed consent was obtained, 5–10 mL of peripheral blood was collected in disposable vacuum tubes for genetic testing. Genomic DNA was extracted from peripheral blood leukocytes using the Wizard genomic DNA purification kit (Promega, Madison, WI, USA).

Targeted Next-Generation Sequencing

We used the online design tool SureDesign to generate a customized HaloPlex target enrichment system (Agilent Technologies, Santa Clara, CA, USA) targeting the regions including *CFTR* exons and 50 base pairs (bp) of flanking introns. The expected coverage of the *CFTR* coding region based on the amplicon design was 99.6 %. The HaloPlex target enrichment system relies on a tailored cocktail of restriction enzymes and customized probes to capture genomic regions of interest, which are subsequently amplified by PCR. Sequencing libraries were prepared according to the manufacturer's instructions. Briefly, genomic DNA was digested with restriction enzymes, followed by hybridization to the biotinylated HaloPlex probe library in the presence of the indexing primer cassette. Hybridization results in the circularization of genomic DNA fragments and incorporation of indices and Illumina sequencing motifs. Hybridized probes were captured with streptavidin-coated magnetic beads. Subsequently, libraries were amplified by PCR to produce a sequencing-ready, target-enriched sample.

All libraries of target-enriched DNA were analyzed on a 2200 TapeStation (Agilent Technologies) to verify successful enrichment. All samples were sequenced on the Illumina MiSeq platform (Illumina Japan, Tokyo, Japan) with paired-end 151-bp reads according to the manufacturer's instruction.

Bioinformatic Analysis of Sequencing Data

The reads were trimmed with the utility program Trim Galore (http://www.bioinformatics.babraham.ac.uk/projects/trim_galore/) to remove possible adapter sequences, based on the Illumina TruSeq adapter index sequences. If either read from a pair was shorter than 20 bp after trimming, that pair was removed from the analysis. The remaining quality reads were mapped to the GRCh37 primary assembly of the human genome (http://ensembl.org/) using the Burrows–Wheeler Alignment tool 0.6.1 (http://bio-bwa.sourceforge.net/). Further sequence data processing, assessment of coverage rates, variant calling, and filtration were performed with the Genome Analysis Toolkit, version 1.6 software (Broad Institute, Cambridge, MA, USA; http://www.broadinstitute.org/gatk/). SNPs and insertions/deletions (indels) were annotated using the ANNOVAR (http://www.openbioinformatics.org/annovar/; BIOBASE, Wolfenbüttel, Germany).

Sanger Sequencing

Sanger sequencing was performed to analyze the DNA sequences which included any nucleotide variant identified by NGS. Exons and adjacent intronic regions of the *CFTR* gene containing the nucleotide variants were amplified by PCR using the primer sets (Table 1). The cycle conditions were as follows: preheating at 95 °C for 5 min, followed by 40 cycles of 95 °C for 30 s, 60 °C for 30 s, and 72 °C for 30 s; and then a final extension at 72 °C for 5 min. PCR products were cleaned up using the Illustra ExoProStar S (GE Healthcare Life Sciences; Little Chalfont, UK). The PCR products were sequenced using an ABI Prism BigDye Terminator Cycle Sequencing Kit, version 3.1 on ABI3730xl DNA Analyzer (Applied Biosystems, Foster City, CA, USA) according to the manufacturer's instructions. The results were compared with the reference sequence derived from the GenBank (http://www.ncbi.nlm.nih.gov/genbank, reference sequence NM_000492) to identify nucleotide substitutions. The A of the ATG start codon was used as nucleotide +1. The mutations are described according to the nomenclature recommended by

Table 1 Primers used for direct sequencing

Exon	Forward	Reverse	Size of PCR product (bp)
2	CCAGAAAAGTTGAATAGTATCA	AAGCAATCCTCTCATCTTGG	369
4	AATTCTCAGGGTATTTTATGAG	CCAGCTCACTACCTAATTTATG	363
10	AGCATCTATTGAAAATATCTGACAAAC	AAAGAGACATGGACACCAAATTAAG	315
11	GGAGGCAAGTGAATCCTGAG	AACCGATTGAATATGGAGCC	343
12	CAGATTGAGCATACTAAAAGTG	CATTTACAGCAAATGCTTGCTAG	224
13	TAGATGACCAGGAAATAGAGA	ATGAGGCGGTGAGAAAAGGT	351
15	GGTGGCATGAAACTGTACTG	TGTATACATCCCCAAACTATCT	251
17	TCAGTAAGTACTTTGGCTGC	CCTATTGATGGTGGATCAGC	390
21	TGTGCCCTAGGAGAAGTGTG	TGACAGATACACAGTGACCCTC	335
23	TATGTCACAGAAGTGATCCC	TGAGTACAAGTATCAAATAGC	252
25	GCTTGAGTGTTTTTAACTCTGTGG	AGACCCCCACACGCAGAC	335
27	CTCTGGTCTGACCTGCCTTC	AGCTCCAATTCCATGAGGTG	334

bp base pairs